

Strong tunable spin-spin coupling with cavity-magnon criticality

Ma-Lei Peng,^{1,*} Miao Tian,^{1,*} Xue-Chun Chen,¹ Guo-Qiang Zhang,^{2,†} Hai-Chao Li,^{3,‡} and Wei Xiong^{1,§}

¹*Department of Physics, Wenzhou University, Zhejiang 325035, China*

²*School of Physics, Hangzhou Normal University, Hangzhou, Zhejiang 311121, China*

³*College of Physics and Electronic Science, Hubei Normal University, Huangshi 435002, China*

(Dated: August 19, 2024)

Strong long-distance spin-spin coupling is desperately demanded for solid-state quantum information processing, but it is still challenged. Here, we propose a hybrid quantum system, consisting of a coplanar waveguide (CPW) resonator weakly coupled to a single nitrogen-vacancy spin in diamond and a yttrium-iron-garnet (YIG) nanosphere holding Kerr magnons, to realize strong long-distance spin-spin coupling. With a strong driving field on magnons, the Kerr effect can squeeze magnons, and thus the coupling between the CPW resonator and the squeezed magnons is *exponentially enhanced*, which produces two cavity-magnon polaritons, i.e., the high-frequency polariton (HP) and low-frequency polariton (LP). When the enhanced cavity-magnon coupling approaches the critical value, the spin is fully decoupled from the HP, while the coupling between the spin and the LP is significantly improved. In the dispersive regime, a strong spin-spin coupling is achieved with accessible parameters. The coupling distance can be up to centimeter scale, limited by the cavity size. Our proposal provides a pave way to manipulate solid spins with cavity-magnon polaritons.

I. INTRODUCTION

Solid spins such as nitrogen-vacancy centers in diamond [1], having good tunability [2] and long coherence time [3–5], are regarded as promising platforms for quantum information science [6, 7]. In particular, strongly coupled spins can, in principle, be used to perform two-qubit operations as required in the spin-based quantum computing scheme [8]. In addition, the spin-spin interaction can be employed to establish the quantum Heisenberg model for the simulation of many-body quantum spin systems [9–12] for discovering intriguing physical phenomena such as discrete time crystals [13] and phantom spin-helix states [14]. However, direct spin-spin coupling is weak due to their small magnetic dipole moments [15–20]. Moreover, the coupling distance is directly determined by their separation. To overcome these, the natural ideal is to look for quantum interfaces [21–34] as bridges to couple long-distance spins, forming diverse hybrid quantum systems [6, 7].

Recently, low-loss magnons, which are the quanta of collective spin excitations in ferromagnetic materials [35–38], have demonstrated significant potential for mediating distant spin-spin coupling [39–44]. Particularly, magnons in the Kittel mode of a yttrium-iron-garnet (YIG) sphere with a nanometer-sized diameter can strongly interact with spins separated by tens of nanometers, enhancing the local magnetic field [39, 40]. Experimentally, magnons in nanomagnets have garnered considerable interest due to advancements in quantum technology [45–51]. This indicates that coupling remote

spins with magnons in nanometer-sized YIG spheres becomes a potential path, and thus offering a route to explore magnon-based quantum information science. To further improve the coupling distance between two spins from nanometer to micrometer, magnons with Kerr effect as quantum interface are theoretically proposed [52]. Also, the YIG nanosphere can be used to realize strong spin-photon coupling in a microwave cavity [53]. Besides these, magnons in a bulk material [42, 43] and thin ferromagnet film [44] have been suggested to coherently couple remote spins. However, achieved strong coupling is severely limited by the distance between two spins.

Motivated by this, we propose a hybrid spin-cavity-magnon system to realize a strong spin-spin coupling with coupling distance~centimeter. In the proposed system, a spin in diamond is located at tens of nanometers from the central line of a coplanar waveguide (CPW) resonator, and weakly coupled to the CPW resonator. The nanometer-sized YIG sphere supporting Kerr magnons (i.e., magnons with Kerr effect) is employed but weakly coupled to the CPW resonator. Experimentally, the strong and tunable magnon Kerr effect, originating from the magnetocrystalline anisotropy [54], has been demonstrated [55], giving rise to bi- and multi-stabilities [55–59], nonreciprocity [60, 61], sensitive detection [62], quantum entanglement [61, 63] and quantum phase transition [64, 65]. Under a strong driving field, this Kerr effect can squeeze magnons, and thus the coupling between magnons and the CPW resonator is exponentially enhanced to the strong coupling regime. The strong magnon-cavity coupling generates two polaritons, i.e., the high-frequency polariton (HP) and the low-frequency polariton (LP). When the enhanced magnon-cavity coupling strength approaches the critical value, the LP becomes critical. Then the coupling between the spin and the HP is fully suppressed in the polariton representation, while the coupling between the spin and the LP is greatly enhanced. By further taking into account the

*These authors equally contributed to the work

†zhangguoqiang@hznu.edu.cn

‡hcl2007@foxmail.com

§xiongweiphys@wzu.edu.cn

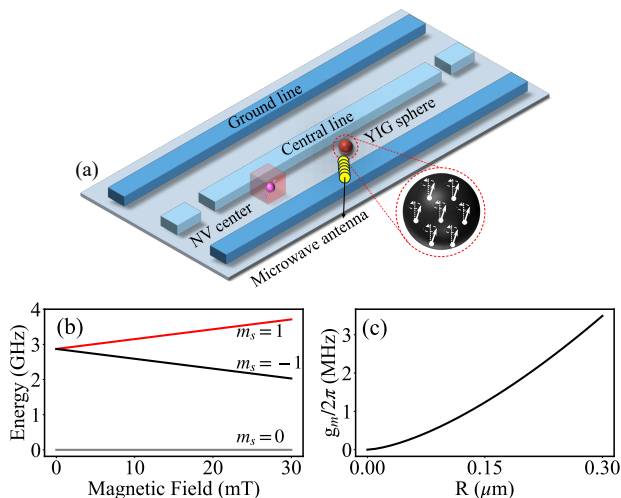


FIG. 1: (a) Schematic diagram of a hybrid quantum system. The single nitrogen vacancy (NV) center spin (pink semi-transparent boxes with a dot), located at d distance away from the central line (light blue strip), is weakly coupled to the CPW resonator (the central part of the central line). The YIG sphere is driven by a microwave field through a microwave antenna, marked in yellow. The dark blue strip denotes the ground line of the CPW resonator. (b) The level structure of the triplet ground state of the NV center, $m_s = 0$ and $m_s = -1$ are selected to form a spin qubit. (c) The cavity-magnon coupling versus the radius R of the YIG nanosphere.

situation of two spins that are dispersively coupled to the LP, an indirect and strong spin-spin coupling can be induced by adiabatically eliminating the degrees of freedom of the LP. Moreover, the achieved strong spin-spin coupling strength is independence of the separation between two spins, it is actually determined by the length of the CPW resonator. Experimentally, the centimeter-sized CPW resonator has been fabricated [66]. As a result, the strong coupling distance between two spins can be up to centimeter scale. Our proposal provides a novel path to remotely manipulate solid spin qubits with critical polaritons in weakly coupled spin-cavity-magnon systems.

II. MODEL AND HAMILTONIAN

We consider a hybrid quantum system consisting of a CPW resonator weakly coupled to both a single NV spin in diamond and a nanometer-sized YIG sphere, as shown in Fig. 1(a). The spin is fabricated far away from the YIG sphere to avoid their direct coupling. In addition, the magnon Kerr effect, stemming from the magnetocrystallographic anisotropy [55, 56], is taken into account. Thus, the total Hamiltonian of the hybrid system can be written as (setting $\hbar = 1$),

$$H_{\text{tot}} = H_{\text{NV}} + H_{\text{CM}} + H_{\text{CS}} + H_K + H_D, \quad (1)$$

where $H_{\text{NV}} = \frac{1}{2}\omega_{\text{NV}}\sigma_z$, with the transition frequency $\omega_{\text{NV}}/2\pi = D - g_e\mu_B B_{\text{ex}}$ between the lowest two levels of the triplet ground state of the NV [see Fig. 1(b)], is the free Hamiltonian of the NV spin. Here, $D = 2.88$ GHz is the zero-field splitting, $g_e = 2$ is the Landé factor, $\mu_B = 14$ MHz/mT is the Bohr magneton, and B_{ex} is the external magnetic field along the crystal axis to lift the near-degenerate states $|m_s = \pm 1\rangle$. Experimentally, the magnetic field can be supplied by a custom-built electromagnet (Tel-Atomic) [67], allowing B_{ex} to vary from a few to hundreds of megahertz [15–17, 67]. The second term

$$H_{\text{CM}} = \omega_c a^\dagger a + g_m (a^\dagger m + a m^\dagger) \quad (2)$$

represents the Hamiltonian of the coupled magnon-cavity subsystem, where ω_c is the frequency of the CPW resonator and g_m is the coupling strength [53], nearly proportional to the radius R of the YIG sphere [see Fig. 1(c)]. Obviously, strong coupling can be obtained by using micrometer-sized sphere, which is widely employed in experiments [68–71]. For the nanometer-sized sphere such as $R \sim 50$ nm, we have $g_m/2\pi \sim 0.2$ MHz, which is much smaller than the typical decay rates of the cavity ($\kappa_c/2\pi \sim 1$ MHz) [72, 73] and Kittel mode ($\kappa_m/2\pi \sim 1$ MHz) [70, 74], i.e., $g_m < \kappa_c, \kappa_m$. This indicates that the coupling between the Kittel mode of the nanosphere and the cavity is in the weak coupling regime, consistent with our assumption.

The Hamiltonian H_{CS} in Eq. (1) describes the interaction between the spin qubit and the cavity. With the rotating-wave approximation, H_{CS} can be governed by [18, 19]

$$H_{\text{CS}} = \lambda (\sigma_+ a + a^\dagger \sigma_-), \quad (3)$$

with the coupling strength $\lambda = g_e\mu_B B_{0,\text{rms}}(d)$ [18], where $B_{0,\text{rms}}(d) = \mu_0 I_{\text{rms}}/2\pi d$ is the magnetic field generated by the vacuum fluctuations of the photons within the CPW resonator, $I_{\text{rms}} = \sqrt{\hbar\omega_c/2L_a}$ is the root-mean-square current flowing through the central line of the CPW resonator when the photon mode is in the ground state, and d is the distance between the spin qubit and the central line of the CPW resonator. Obviously, the root mean square current induced magnetic field is dependence of the distance d . To estimate λ , $\omega_c/2\pi \sim 6.78$ GHz and $L_a \sim 2$ nH [72] are chosen. For $d \sim 5$ μm , we have $B_{0,\text{rms}} \sim 2.5 \times 10^{-10}$ T and $\lambda/2\pi \sim 70$ Hz. When $d \sim 50$ nm, $B_{0,\text{rms}} \sim 2.5 \times 10^{-7}$ T is estimated, giving rise to $\lambda/2\pi \sim 7$ kHz [18]. This indicates that the coupling between the spin qubit and the cavity is also in the weak coupling regime, where $\lambda < \kappa_c$. Due to this fact, we here assume that the spin qubit is placed close to the central line of the CPW resonator to obtain a moderate coupling strength, although it is still weakly coupled to the cavity. Experimentally, such weak spin-cavity couplings can be measured.

The Hamiltonian H_K in Eq. (1) denotes the magnon Kerr effect, characterizing the coupling among magnons

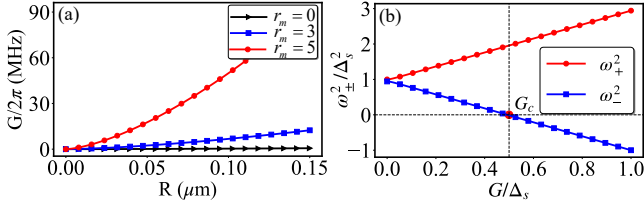


FIG. 2: (a) The coupling strength between the squeezed magnons and the CPW resonator versus the radius of the YIG nanosphere with different squeezing parameters $r_m = 0, 3, 5$. (b) The square of polariton frequencies versus the coupling between the squeezed magnons and the CPW resonator.

in the YIG sphere and provides the anharmonicity of the magnons, which is given by [56]

$$H_K = \omega_m m^\dagger m + K m^\dagger m^\dagger m m, \quad (4)$$

where $\omega_m = \gamma B_0 - 2\mu_0 K_{\text{an}} \gamma^2 s / M^2 V_m + \mu_0 K_{\text{an}} \gamma^2 / M^2 V_m$ is the frequency of the Kittel mode, with the gyromagnetic ratio $\gamma/2\pi = g_e \mu_B / \hbar = 28 \text{ GHz/T}$, the vacuum permeability μ_0 , the first-order anisotropy constant of the YIG sphere K_{an} , the amplitude of a bias magnetic field B_0 , the saturation magnetization M , the volume of the YIG sphere V_m , and $s = 1/2$ is the spin quantum number. $K = \mu_0 K_{\text{an}} \gamma^2 / M^2 V_m$ is the coefficient. Experimentally, the bias magnetic field can be generated by a superconducting magnet to magnetize the YIG sphere, and it is tunable in the range of 0 to 1 T, so the given frequency of the magnons in the Kittel mode ranges from several hundreds of megahertz to 28 GHz [55]. We here take the experimentally accessible value $B_0 = 98.5 \text{ mT}$ for achieving $\omega_m/2\pi = 2.6 \text{ GHz}$. Other parameters are $\mu_0 K_{\text{an}} = 2480 \text{ J/m}^3$, $M = 196 \text{ kA/m}$ [54]. Apparently, the Kerr coefficient is inversely proportional to the volume of the YIG sphere, i.e., $K \propto 1/V_m$, the Kerr effect can become significantly important for a YIG nanosphere. For example, when $R \sim 50 \text{ nm}$, $K/2\pi \sim 128 \text{ Hz}$, but $K/2\pi \sim 0.05 \text{ nHz}$ for $R \sim 0.5 \text{ mm}$ (the usual size of the YIG sphere used in various previous experiments). Obviously, K is much smaller in the latter case. Because our proposal mainly relies on the Kerr effect, we here use the nanometer-sized YIG sphere to obtain a strong Kerr effect. The last term

$$H_D = \Omega_d (m^\dagger e^{-i\omega_d t} + m e^{i\omega_d t}). \quad (5)$$

in Eq. (1) describes the interaction between the Kittel mode and the driving field, where Ω_d is the Rabi frequency and ω_d is the frequency of the driving field. In the rotating frame with respect to the driving frequency (ω_d), the total Hamiltonian in Eq. (1) becomes

$$H_{\text{sys}} = \frac{1}{2} \Delta_{\text{NV}} \sigma_z + \Delta_c a^\dagger a + H'_K + \Omega_d (m^\dagger + m) + \lambda (\sigma_+ a + a^\dagger \sigma_-) + g_m (a^\dagger m + a m^\dagger), \quad (6)$$

where $\Delta_{\text{NV}} = \omega_{\text{NV}} - \omega_d$ is the frequency detuning of the spin qubit from the driving field, $\Delta_c = \omega_c - \omega_d$ is the frequency detuning of the cavity field from the driving field,

and $H'_K = \delta_m m^\dagger m + K m^\dagger m^\dagger m m$ [52], with $\delta_m = \omega_m - \omega_d$ being the frequency detuning of the Kittel mode from the driving field. Due to the large Ω_d , the Hamiltonian H_{sys} in Eq. (6) can be linearized by writing each system operator as the expectation value plus its fluctuation [75]. By neglecting the higher-order fluctuation terms, Eq. (6) is linearize as

$$H_{\text{lin}} = \frac{1}{2} \Delta_{\text{NV}} \sigma_z + \Delta_c a^\dagger a + \mathcal{H}_K + \lambda (\sigma_+ a + a^\dagger \sigma_-) + g_m (a^\dagger m + a m^\dagger), \quad (7)$$

with

$$\mathcal{H}_K = \Delta_m m^\dagger m + K_s (m^2 + m^{\dagger 2}), \quad (8)$$

where the effective magnon frequency detuning $\Delta_m = \delta_m + 4K|\langle m \rangle|^2$ is induced by the Kerr effect, which has been demonstrated experimentally [55, 56]. The amplified coefficient $K_s = K\langle m \rangle^2$ is the effective strength of the two-magnon process, which can give rise to squeeze magnons in the Kittel mode. Aligning the biased magnetic field along the crystalline axis [100] ([110]) of the YIG sphere [54, 56], K is positive (negative), and thus we have $K_s > 0$ ($K_s < 0$). To achieve our goal of interest, we take $K_s < 0$ below. The linearized Kerr Hamiltonian \mathcal{H}_K in Eq. (8) describes the two-magnon process, which can give rise to the magnon squeezing.

Below we operate the proposed hybrid system in the magnon-squeezing frame by diagonalizing the Hamiltonian \mathcal{H}_K with the Bogoliubov transformation $m = m_s \cosh(r_m) + m_s^\dagger \sinh(r_m)$, where $r_m = \frac{1}{4} \ln \frac{\Delta_m - 2K_s}{\Delta_m + 2K_s}$ is the squeezing parameter. After diagonalization, \mathcal{H}_K becomes

$$\mathcal{H}_{\text{KS}} = \Delta_s m_s^\dagger m_s \quad (9)$$

with $\Delta_s = \sqrt{\Delta_m^2 - 4K_s^2}$ being the frequency of the squeezed magnons, and Eq. (7) is transformed to

$$H_S = \frac{1}{2} \Delta_{\text{NV}} \sigma_z + H_{\text{CMS}} + \lambda (\sigma_+ a + a^\dagger \sigma_-), \quad (10)$$

where

$$H_{\text{CMS}} = \Delta_c a^\dagger a + \Delta_s m_s^\dagger m_s + G (a^\dagger + a) (m_s^\dagger + m_s) \quad (11)$$

is the effective Hamiltonian of the CPW resonator coupled to the squeezed magnons, $G = \frac{1}{2} g_m e^{r_m}$ is the exponentially enhanced coupling strength between the squeezed magnons and the CPW resonator. Because both the parameters Δ_m and K_s can be tuned, so r_m can be very large when $\Delta_m \sim -2K_s$, leading to the strong G even for nanometer-sized YIG sphere [see curves in Fig. 2(a)]. Specifically, when $r_m = 0$, i.e., magnons in the Kittel mode is not squeezed, the coupling strength between the CPW resonator and the Kittel mode is unamplified, giving rise to weak G [see the black curve in Fig. 2(a)]. When magnons in the Kittel mode are

squeezed but with moderate squeezing parameters such as $r_m = 3$ and $r_m = 5$, we find the coupling strength G can be significantly improved for the YIG nanosphere. For example, $R \sim 50$ nm and $r_m \sim 3$, we have $G/2\pi = 2$ MHz, which is comparable with the decay rates of the CPW resonator (κ_c) and the Kittel mode (κ_m). But when $r_m \sim 5$, $G/2\pi = 17$ MHz, which is much larger than both κ_c and κ_m . These indicate that strong coupling can be realized by tuning the squeezing parameter r_m . In addition, G can be further enhanced by using the larger radius of the YIG sphere when r_m is fixed. Once the strong coupling between the squeezed magnons and the CPW resonator is achieved, the counter-rotating terms $\propto a^\dagger m_s^\dagger$ and am_s in Eq. (11) are related to two-mode squeezing, while rotating terms $\propto a^\dagger m_s$ and am_s^\dagger allow quantum state transfer between the squeezed magnons and the CPW resonator. By combining these, polaritons with criticality can be formed, as shown below.

III. STRONG COUPLING BETWEEN THE SINGLE NV SPIN AND THE LOW-FREQUENCY POLARITON

By further diagonalizing the Hamiltonian H_{CMS} in Eq. (11), two polaritons with eigenfrequencies

$$\omega_\pm^2 = \frac{1}{2} \left[\Delta_c^2 + \Delta_s^2 \pm \sqrt{(\Delta_c^2 - \Delta_s^2)^2 + 16G^2 \Delta_c \Delta_s} \right] \quad (12)$$

can be obtained. This is owing to the fact of the achieved strong coupling between the squeezed magnons and the CPW resonator. For convenience, we call two polaritons with frequencies ω_+ and ω_- as the high- and low-frequency polaritons (HP and LP). The diagonalized H_{CMS} reads

$$H_{\text{diag}} = \omega_+ a_+^\dagger a_+ + \omega_- a_-^\dagger a_-, \quad (13)$$

where

$$a = \frac{\cos \theta}{2\sqrt{\Delta_c \omega_-}} \left[a_- (\Delta_c + \omega_-) + a_-^\dagger (\Delta_c - \omega_-) \right] + \frac{\sin \theta}{2\sqrt{\Delta_c \omega_+}} \left[a_+ (\Delta_c + \omega_+) + a_+^\dagger (\Delta_c - \omega_+) \right]. \quad (14)$$

Substituting Eqs. (13) and (14) into Eq. (10), the Hamiltonian of the spin coupled to cavity-magnon polaritons can be given by

$$H_{\text{CMP}} = \frac{1}{2} \Delta_{\text{NV}} \sigma_z + \omega_+ a_+^\dagger a_+ + \omega_- a_-^\dagger a_- + g_+ (\sigma_+ a_- + \sigma_- a_-^\dagger) + g_- (\sigma_+ a_-^\dagger + \sigma_- a_-) + g'_+ (\sigma_+ a_+ + \sigma_- a_+^\dagger) + g'_- (\sigma_+ a_+^\dagger + \sigma_- a_+), \quad (15)$$

where $g_\pm = \lambda \cos \theta (\Delta_c \pm \omega_-) / 2\sqrt{\Delta_c \omega_-}$ denote the effective coupling strength between the NV spin and the

LP, $g'_\pm = \lambda \sin \theta (\Delta_c \pm \omega_+) / 2\sqrt{\Delta_c \omega_+}$ represent the effective coupling strength between the NV spin and the HP. Obviously, both g_\pm and g'_\pm can be *tuned* by the driving field on the Kittel mode of the YIG sphere. The parameter θ is defined by $\tan(2\theta) = 4G\sqrt{\Delta_c \Delta_s} / (\Delta_c^2 - \Delta_s^2)$. To show the behavior of two polaritons with the coupling strength G , we plot the square of polariton frequencies versus the coupling strength G in Fig. 2(b). Clearly, one can see that ω_+^2 increases with G , but ω_-^2 decreases. When $\omega_-^2 = 0$, G reduces to the critical coupling strength G_c , i.e.,

$$G = G_c \equiv \frac{1}{2} \sqrt{\Delta_c \Delta_s}, \quad (16)$$

which means ω_- is real for $G < G_c$, while ω_- is imaginary (the low-polariton is unstable) for $G > G_c$. When we operate the coupled cavity-magnon subsystem around the critical point (i.e., $G \rightarrow G_c$) and $\Delta_c \gg \Delta_s$ is satisfied, we have $g_+ \approx g_- \rightarrow \frac{1}{2} \lambda \sqrt{\Delta_c / \omega_-}$, $g'_+ \approx g'_- \rightarrow 0$. Due to the large Δ_c and the extremely small ω_- , $g_+ \approx g_- \gg \lambda$. These indicate that coupling between the NV spin and the HP can be completely suppressed, while the coupling between the NV spin and the LP is significantly enhanced. By choosing $\Delta_c = 4 \times 10^3 \omega_-$ with $\omega_- / 2\pi = 1.6$ MHz, $g_+ = g_- \sim 10\sqrt{10}\lambda$ are estimated. Using $d = 50$ nm, $\lambda = 2\pi \times 7$ kHz is obtained, resulting in $g_+ / 2\pi \sim 0.22$ MHz. This suggests that the coupling between the spin and the LP can be in the strong coupling regime. In principle, g_\pm can be further enhanced by using the larger Δ_c or much smaller ω_- . Note that both the decay rates of the squeezed magnons and CPW resonator are not considered in the above analyses. When taking them into account, the critical coupling strength $G_c = \frac{1}{2} \sqrt{\Delta_c \Delta_s}$ is shifted to $G'_c = \frac{1}{2} \sqrt{(\Delta_c^2 + \kappa_c^2)(\Delta_s^2 + \kappa_0^2) / \Delta_c \Delta_s}$ [27, 76], where we assume that the decay rates of the squeezed magnon mode (κ_m) and the CPW resonator (κ_c) are equal, i.e., $\kappa_m = \kappa_c = \kappa_0$. At the new critical point, the coupling strength g_+ (g_-) can still be enhanced to the strong coupling regime. When the condition $\Delta_{\text{NV}} \geq \omega_- \gg g_\pm$ is ensured, the rotating-wave approximation can be safely applied to Eq. (15), as numerically demonstrated in Fig. 3. To satisfy this condition, the frequency of the driving field $\omega_d / 2\pi = 2.598$ GHz is taken and the external magnetic field is tuned to be $B_{\text{ex}} = 10$ mT for having $\omega_{\text{NV}} / 2\pi = 2.6$ GHz and $\Delta_{\text{NV}} / 2\pi = 1.6$ MHz. Under the rotating-wave approximation, Eq. (15) reduces to

$$H_{\text{JC}} = \frac{1}{2} \Delta_{\text{NV}} \sigma_z + \omega_- a_-^\dagger a_- + g_+ (\sigma_+ a_- + \sigma_- a_-^\dagger), \quad (17)$$

which is the so-called Jaynes-Cummings model with the strong coupling g_+ , allowing quantum state exchange between the spin and the LP, as demonstrated in Fig. 4(a), where the spin is initially prepared in the excited state and the LP is in the ground state.

When dissipations are included, the dynamics of the

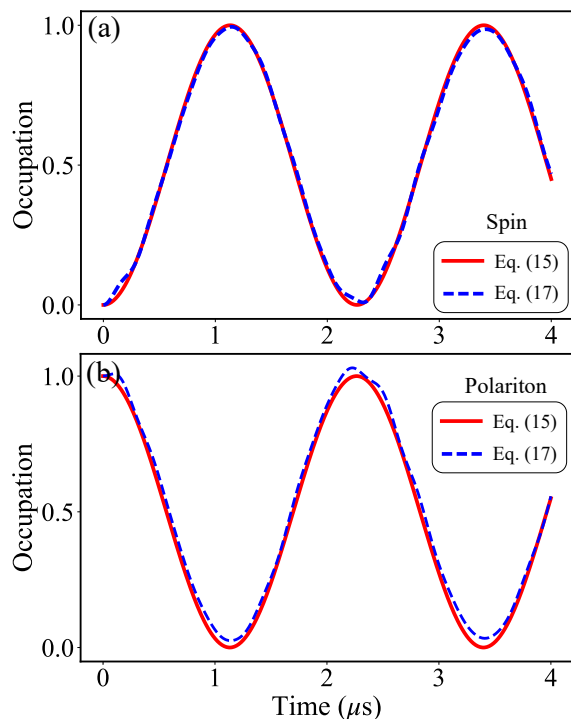


FIG. 3: (a) Simulating the expectation of the spin qubit with Eqs. (15) and (17). (b) Simulating the expectation of the LP formed by the squeezed magnons and photons with Eqs. (15) and (17). The simulation results are respectively denoted by the solid red and dashed blue curves in (a) and (b). Here, the spin qubit is initially prepared in the ground state and the LP is in the excited state, and the coupling strength is $g_+/2\pi = 0.22$ MHz.

system can be described by the master equation,

$$\frac{d\rho}{dt} = -i[H_{\text{JC}}, \rho] + \kappa_- \mathcal{D}[a_-] \rho + \gamma_{\perp} \mathcal{D}[\sigma_-] \rho + \gamma_{\parallel} \mathcal{D}[\sigma_z] \rho, \quad (18)$$

where $\mathcal{D}[o]\rho = o\rho o^{\dagger} - \frac{1}{2}(o^{\dagger}o\rho + \rho o^{\dagger}o)$, and γ_{\perp} (γ_{\parallel}) is the transversal (longitudinal) relaxation rate of the NV spin [77], κ_- is the decay rate of the LP. In Fig. 4(b), we use the qutip package in python [78, 79] to numerically simulate the dynamics of the spin and LP governed by Eq. (18). The results show that state exchange between the spin and the LP can be realized in the presence of dissipations such as $\kappa_-/2\pi \sim 1$ MHz and $\gamma_{\perp}/2\pi \sim 1$ kHz [80], although the occupation probability decreases with long evolution time. For the NV spins, the longitudinal relaxation is usually much smaller than the transversal relaxation experimentally [77], i.e., $\gamma_{\parallel} \ll \gamma_{\perp}$, thus the last term related to the longitudinal relaxation of the spin qubit can be safely neglected. Even when it is included, only the negligible effects on the dynamics of the LP and the spin qubit in Fig. 4(b) are introduced, which can be numerically checked.

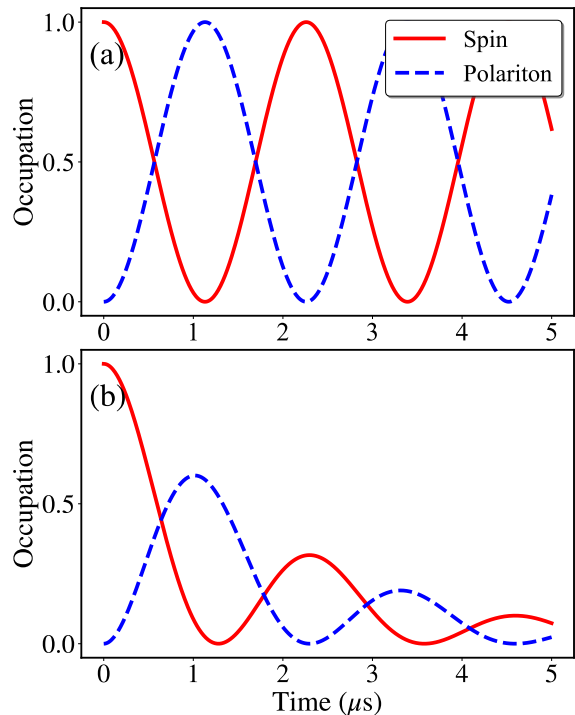


FIG. 4: The occupation of the LP and spin qubit versus the evolution time at $G \rightarrow G_c$ and $\Delta_c \gg \Delta_s$ (a) without and (b) with dissipations. The spin decay rate is $\gamma_{\perp}/2\pi \sim 1$ kHz and the LP decay rate is $\kappa_-/2\pi \sim 1$ MHz. In both (a) and (b), the spin qubit is initially prepared in the excited state and the LP is in the ground state, and the coupling strength is $g_+/2\pi = 0.22$ MHz.

IV. THE EFFECTIVE STRONG COUPLING BETWEEN TWO SINGLE NV SPINS

Here, we further consider the case that two identical NV spins are symmetrically placed away from the YIG sphere in the CPW resonator. Thus, two spins interact with the CPW resonator with the same coupling strength λ . By operating the cavity-magnon subsystem around the critical point, the couplings between two spins and the HP can be fully suppressed, while the couplings between two spins and the LP are greatly enhanced, similar to the single spin case. Therefore, the Hamiltonian of the hybrid system with two identical spins can be effectively described by Tavis-Cummings model,

$$H_{\text{TC}} = \omega_- a_-^{\dagger} a_- + \frac{1}{2} \Delta_{\text{NV}} \left(\sigma_z^{(1)} + \sigma_z^{(2)} \right) + g_+ \left[\left(\sigma_+^{(1)} + \sigma_+^{(2)} \right) a_- + \text{h.c.} \right]. \quad (19)$$

To enter the dispersive regime, i.e., $|\Delta_{\text{NV}} - \omega_-| \gg g_+$, we can further tune the external magnetic field B_{ex} to have $\Delta_{\text{NV}}/2\pi = 16$ MHz. In this regime, the LP can be as an interface to induce an indirect coupling between two spins by using the Fröhlich-Nakajima transformation [81, 82]. Specifically, We first rewrite H_{TC} in Eq. (19) as H_0 plus

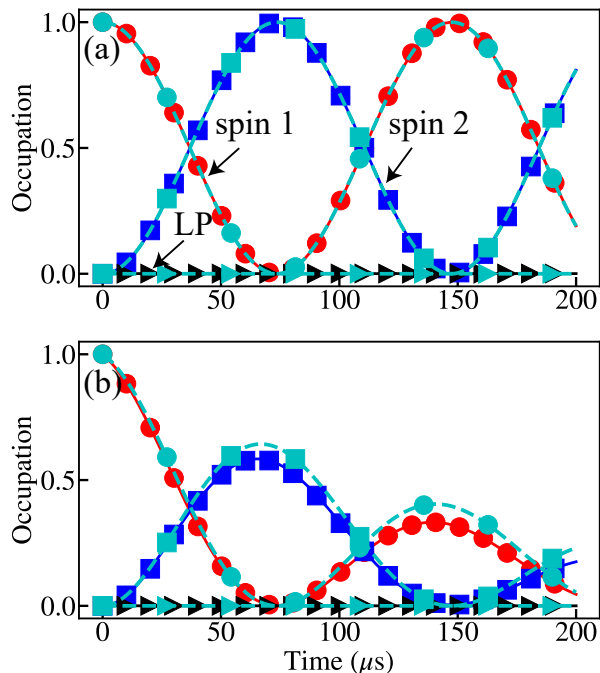


FIG. 5: The occupation of two spins and the LP versus the evolution time in the dispersive regime (a) without and (b) with dissipations. The curves in cyan are simulated with the effective Hamiltonian in Eq. (23). Other colored curves are simulated with the original Hamiltonian in Eq. (19). The parameters $\omega_-/2\pi = 1.6$ MHz, $\Delta_{\text{NV}}/2\pi = 16$ MHz, and $g_+/2\pi = 0.22$ MHz are used.

H_I , where

$$\begin{aligned} H_0 &= \omega_- a_-^\dagger a_- + \frac{1}{2} \Delta_{\text{NV}} (\sigma_z^{(1)} + \sigma_z^{(2)}) \\ H_I &= g_+ \left[(\sigma_+^{(1)} + \sigma_+^{(2)}) a_- + \text{h.c.} \right]. \end{aligned} \quad (20)$$

Then we choose the operator V , related to the transformation $U = \exp(-V)$, to satisfy

$$[H_0, V] + H_I = 0, \quad (21)$$

where

$$V = \frac{g_+}{\Delta_{\text{NV}} - \omega_-} (a_-^\dagger \sigma_-^{(1)} + a_-^\dagger \sigma_-^{(2)}) - \text{h.c.} \quad (22)$$

Applying the unitary transformation with the unitary operator U to the Hamiltonian H_{TC} in Eq. (19) and up to the second order in g_+/Δ_{NV} , the spin qubits are decoupled from the LP. By adiabatically eliminating the degrees of freedom of the LP, we can obtain the effective spin-spin Hamiltonian as

$$H_{\text{eff}} = \frac{1}{2} \omega_{\text{eff}} (\sigma_z^{(1)} + \sigma_z^{(2)}) + g_{\text{eff}} (\sigma_+^{(1)} \sigma_-^{(2)} + \sigma_-^{(1)} \sigma_+^{(2)}), \quad (23)$$

where $\omega_{\text{eff}} = \Delta_{\text{NV}} + 2g_{\text{eff}} n_- + g_{\text{eff}}$ is the effective transition frequency of the NV spin, depending on the

mean occupation number $n_- = \langle a_-^\dagger a_- \rangle$ of the LP, $g_{\text{eff}} = -g_+^2/(\Delta_{\text{NV}} - \omega_-)$ is the effective spin-spin coupling strength induced by the LP. To estimate g_{eff} , we assume the distance between the spin and the central line of the CPW resonator $d = 50$ nm, so $g_+/2\pi = 0.22$ MHz, thus we have $g_{\text{eff}}/2\pi = 3.4$ kHz at $\Delta_{\text{NV}}/2\pi = 16$ MHz. Obviously, $g_{\text{eff}} > \gamma_\perp (\sim 1$ kHz), i.e., the strong spin-spin coupling is achieved. This can be directly demonstrated by simulating the dynamics of the effective system, governed by Eq. (23) or Eq. (19) in the dispersive regime, with the master equation. The simulating results are presented in Fig. 5. Without dissipation, the simulation results with Eq. (19) and Eq. (23) matches well. With dissipation, we show that a slight discrepancy between the outcomes obtained by Eq. (19) and Eq. (23) is predicted, which is caused by the neglected high-order terms in Eq. (23). One can see that quantum states of two spins can be exchanged each other with [see Fig. 5(a)] and without [see Fig. 5(b)] dissipations, while the LP is always in the initial state. Note that the achieved strong spin-spin coupling is not limited by the separation between two spins, it is only determined by the length of the CPW resonator. Experimentally, the centimeter-sized cavity has been fabricated [66], so the strong spin-spin coupling distance can be increased to centimeters. Compared to previous proposals of directly coupled spins to a YIG nanosphere [39–41], the distance here is nearly enhanced by *six* orders of magnitude.

V. CONCLUSION AND DISCUSSION

It is noteworthy that our proposal involves various types of magnetic fields serving different purposes. For magnons in the Kittel mode, a static magnetic field B_0 is essential. To lift the degeneracy between two excited levels of the NV spin, an external magnetic field B_{ex} is required. When coupling the NV spin to the CPW resonator, a magnetic field B_{orrms} induced by the root-mean-square current becomes necessary. This current is solely determined by the frequency and inductance of the CPW resonator and thus B_{orrms} is unaffected by B_0 and B_{ex} . In addition, by remotely separating the NV spin and the YIG sphere, the mutual influence between B_0 and B_{ex} can also be avoided. Besides, the Kittel mode of the YIG sphere can be driven by a local microwave field via a loop antenna connected to a superconducting microwave line. This technology has been used to demonstrate the magnon Kerr effect and the bistability of the cavity-magnon polariton [55, 56]. Experimentally, the biased magnetic field of the magnons, the magnetic component of the microwave drive field, and the magnetic field of the cavity can be nearly perpendicular to one another at the site of the small YIG sphere. Thus, the applied driving field can be used to efficiently manipulate the magnons and gives rise to negligible effects on both the cavity and the remote diamond spins.

In summary, we have proposed a hybrid system con-

sisting of a CPW resonator weakly coupled to NV spins and a YIG nanosphere supporting magnons with the Kerr effect. With a strong driving field, the Kerr effect can squeeze magnons, giving rise to an exponentially enhanced strong cavity-magnon coupling, and thus cavity-magnon polaritons can be formed. When the cavity-magnon coupling strength reaches the critical value, the spin-LP coupling is greatly enhanced to the strong coupling regime with accessible parameters, while the coupling between the spin and the HP is fully suppressed. Using the LP as quantum interface in the dispersive regime, the strong long-distance spin-spin coupling can be achieved, which allows quantum state exchange between two spins. With current fabricated technology of the CPW resonator, the distance of the strong spin-spin coupling can be up to centimeter scale, which is improved about six orders of magnitude more than the previous proposal of directly coupled spins to the YIG nanosphere. Our scheme provides a potential path to realize a long-distance strong spin-spin coupling with critical cavity-magnon polaritons in weakly coupled hybrid systems.

Funding. Zhejiang Provincial Natural Science Foundation of China under Grant No. LY24A040004, National Natural Science Foundation of China (Grants No. 11804074, No. 12205069, No. 11904201).

Disclosures. The authors declare no conflicts of interest.

Data Availability. The data that support the findings of this study are available from the corresponding author upon reasonable request.

APPENDIX

In this appendix, we give the relationship among the mean magnon number $N_m = |\langle m \rangle|^2$, the effective magnon frequency detuning Δ_m , the magnon decay rate κ_m , and the Rabi frequency of the driving field Ω_d . Also,

the value of Ω_d is estimated with accessible parameters. Starting from Eq. (6) in the main text, the dynamics of magnons can be governed by the quantum Langevin equation:

$$\frac{dm}{dt} = -(\kappa_m + i\delta_m)m - 2iKm^\dagger mm - i\Omega_d, \quad (\text{A1})$$

where the term related to the CPW resonator is neglected due to its weak interaction with the Kittel mode. As we are interested in the steady-state solution, the vacuum input noise with zero mean value is also omitted in Eq. (A1). In a long-time limit, the system reaches its steady state, thus we have $d\langle m \rangle/dt = 0$, i.e.,

$$\langle m \rangle = -\frac{i\Omega_d}{\kappa_m + i(\Delta_m - 2K_s)}. \quad (\text{A2})$$

For obtaining a large squeezing parameter r_m , $\Delta_m \sim -2K_s$ should be satisfied. Using this condition, Eq. (A2) reduces to

$$\langle m \rangle = -\frac{i\Omega_d}{\kappa_m + 2i\Delta_m}, \quad (\text{A3})$$

and so the mean magnon number is

$$N_m = \frac{\Omega_d^2}{\kappa_m^2 + 4\Delta_m^2}. \quad (\text{A4})$$

In the main text, we take the frequencies of the Kittel mode and the driving field as $\omega_m/2\pi = 2.6$ GHz and $\omega_d/2\pi = 2.598$ GHz, respectively. Thus, the detuning from the Kittel mode to the driving field is $\delta_m/2\pi = (2.6 - 2.598)$ GHz = 2 MHz. From the squeezing condition $\Delta_m = \delta_m + 4K_s = -2K_s$, one can obtain $K_s = -\delta_m/6 = -2\pi \times 0.33$ MHz. For $K/2\pi = 128$ Hz, the mean magnon number $N_m = K_s/K \approx 0.26 \times 10^4$ is estimated. From Eq. (A4), we have $\Omega_d/2\pi \approx 2\Delta_m\sqrt{N_m}/2\pi = 66$ MHz.

-
- [1] R. Schirhagl, K. Chang, M. Loretz, and C. L. Degen, Nitrogen-Vacancy Centers in Diamond: Nanoscale Sensors for Physics and Biology, *Annu. Rev. Phys. Chem.* **65**, 83 (2014).
 - [2] M. W. Doherty, N. B. Manson, P. Delaney, F. Jelezko, J. Wrachtrup, L. C. L. Hollenberg, The nitrogen-vacancy colour centre in diamond, *Phys. Rep.* **528**, 1 (2013).
 - [3] N. Bar-Gill, L. Pham, A. Jarmola, D. Budker, and R. Walsworth, Solid-state electronic spin coherence time approaching one second. *Nat. Commun.* **4**, 1743 (2013).
 - [4] F. Jelezko, T. Gaebel, I. Popa, A. Gruber, and J. Wrachtrup, Observation of Coherent Oscillations in a Single Electron Spin, *Phys. Rev. Lett.* **92**, 076401 (2004).
 - [5] G. Balasubramian, P. Neumann, D. Twitchen, M. Markham, R. Koslov, N. Mizuochi, J. Isoya, J. Achard, J. Beck, J. Tissler, V. Jacques, P. R. Hemmer, F. Jelezko, and J. Wrachtrup, Ultralong spin coherence time in isotopically engineered diamond, *Nat. Mater.* **8**, 383 (2009).
 - [6] Z. L. Xiang, S. Ashhab, J. Q. You, and F. Nori, Hybrid quantum circuits: Superconducting circuits interacting with other quantum systems, *Rev. Mod. Phys.* **85**, 623 (2013).
 - [7] G. Kurizki, P. Bertet, Y. Kubo, K. Mølmer, D. Petrosyan, P. Rabl, and J. Schmiedmayer, Quantum technologies with hybrid systems, *Proc. Natl. Acad. Sci. USA* **112**, 3866 (2015).
 - [8] D. Loss and D. P. DiVincenzo, *Phys. Rev. A* **57**, 120 (1998).
 - [9] Y. Salathé, M. Mondal, M. Oppliger, J. Heinsoo, P. Kurpiers, A. Potočnik, A. Mezzacapo, U. Las Heras, L. Lamata, E. Solano, S. Filipp, and A. Wallraff, Digital quantum simulation of spin Models with circuit quantum electrodynamics. *Phys. Rev. X* **5**, 021027 (2015).
 - [10] L. Savary, and L. Balents, Quantum spin liquids: a review. *Rep. Prog. Phys.* **80**, 016502 (2016).
 - [11] H. Bernien, S. Schwartz, A. Keesling, H. Levine, A. Om-

- ran, H. Pichler, S. Choi, A. S. Zibrov, M. Endres, M. Greiner, V. Vuletić, and M. D. Lukin, Probing many-body dynamics on a 51-atom quantum simulator. *Nature* **551**, 579 (2017).
- [12] P. N. Jepsen, J. Amato-Grill, I. Dimitrova, W. W. Ho, E. Demler, and W. Ketterle, Spin transport in a tunable Heisenberg model realized with ultracold atoms. *Nature* **588**, 403 (2020).
- [13] J. Zhang, P. W. Hess, A. Kyprianidis, P. Becker, A. Lee, J. Smith, G. Pagano, I.-D. Potirniche, A. C. Potter, A. Vishwanath, N. Y. Yao, and C. Monroe, Observation of a discrete time crystal. *Nature* **543**, 217 (2017).
- [14] P. N. Jepsen, Y. K. ‘Eunice’ Lee, H. Lin, I. Dimitrova, Y. Margalit, W. W. Ho, and W. Ketterle Long-lived phantom helix states in Heisenberg quantum magnets. *Nat. Phys.* **18**, 899 (2022).
- [15] Y. Kubo, F. R. Ong, P. Bertet, D. Vion, V. Jacques, D. Zheng, A. Dréau, J.-F. Roch, A. Auffeves, F. Jelezko, J. Wrachtrup, M. F. Barthe, P. Bergonzo, and D. Esteve, Strong Coupling of A Spin Ensemble to A Superconducting Resonator, *Phys. Rev. Lett.* **105**, 140502 (2010).
- [16] D. Marcos, M. Wubs, J. M. Taylor, R. Aguado, M. D. Lukin, and A. S. Sørensen, Coupling Nitrogen-Vacancy Centers in Diamond to Superconducting Flux Qubits, *Phys. Rev. Lett.* **105**, 210501 (2010).
- [17] X. Zhu, S. Saito, A. Kemp, K. Kakuyanagi, S. Karimoto, H. Nakano, W. J. Munro, Y. Tokura, M. S. Everitt, K. Nemoto, M. Kasu, N. Mizuochi, and K. Semba, Coherent coupling of a superconducting flux qubit to an electron spin ensemble in diamond, *Nature (London)* **478**, 221 (2011).
- [18] J. Twamley and S. D. Barrett, Superconducting cavity bus for single nitrogen-vacancy defect centers in diamond, *Phys. Rev. B* **81**, 241202(R) (2010).
- [19] W. Xiong, J. Chen, B. Fang, M. Wang, L. Ye, and J. Q. You, Strong tunable spin-spin interaction in a weakly coupled nitrogen vacancy spin-cavity electromechanical system, *Phys. Rev. B* **103**, 174106 (2021).
- [20] W. Xiong, J. Chen, B. Fang, C. H. Lam, and J. Q. You, Coherent perfect absorption in a weakly coupled atom-cavity system, *Phys. Rev. A* **101**, 063822 (2020).
- [21] P. B. Li, Z. L. Xiang, P. Rabl, and F. Nori, Hybrid Quantum Device with Nitrogen-Vacancy Centers in Diamond Coupled to Carbon Nanotubes, *Phys. Rev. Lett.* **117**, 015502 (2016).
- [22] M. Ściesiek, K. Sawicki, W. Pacuski, K. Sobczak, T. Kazimierczuk, A. Gólnik, and J. Suffczyński, Long-distance coupling and energy transfer between exciton states in magnetically controlled microcavities, *Commun Mater* **1**, 78 (2020).
- [23] P. Rabl, S. J. Kolkowitz, F. H. L. Koppens, J. G. E. Harris, P. Zoller, and M. D. Lukin, A quantum spin transducer based on nanoelectromechanical resonator arrays, *Nat. Phys.* **6**, 602 (2010).
- [24] L. Tian, Robust Photon Entanglement via Quantum Interference in Optomechanical Interfaces, *Phys. Rev. Lett.* **110**, 233602 (2013).
- [25] J. Chen, Z. Li, X. Q. Luo, W. Xiong, M. Wang, H. C. Li, Strong single-photon optomechanical coupling in a hybrid quantum system, *Opt. Express* **29**, 32639 (2021).
- [26] M. Aspelmeyer, T. J. Kippenberg, and F. Marquardt, Cavity optomechanics, *Rev. Mod. Phys.* **86**, 1391 (2014).
- [27] W. Xiong, M. Wang, G. Q. Zhang, and J. Chen, Optomechanical-interface-induced strong spin-magnon coupling, *Phys. Rev. A* **107**, 033516 (2023).
- [28] W. Xiong, Z. Li, Y. Song, J. Chen, G. Q. Zhang, and M. Wang, Higher-order exceptional point in a pseudo-Hermitian cavity optomechanical system, *Phys. Rev. A* **104**, 063508 (2021).
- [29] W. Xiong, Z. Li, G. Q. Zhang, M. Wang, H. C. Li, X. Q. Luo, and J. Chen, Higher-order exceptional point in a blue-detuned non-Hermitian cavity optomechanical system, *Physical Review A* **106**, 033518 (2022).
- [30] S. D. Bennett, N. Y. Yao, J. Otterbach, P. Zoller, P. Rabl, and M. D. Lukin, Phonon-Induced Spin-Spin Interactions in Diamond Nanostructures: Application to Spin Squeezing, *Phys. Rev. Lett.* **110**, 156402 (2013).
- [31] P. B. Li, Y. Zhou, W. B. Gao, and F. Nori, Enhancing Spin-Phonon and Spin-Spin Interactions Using Linear Resources in a Hybrid Quantum System, *Phys. Rev. Lett.* **125**, 153602 (2020).
- [32] P. Ovarthaiyapong, K. W. Lee, B. A. Myers, and A. C. Bleszynski Jayich, Dynamic strain-mediated coupling of a single diamond spin to a mechanical resonator. *Nat. Commun.* **5**, 4429 (2014).
- [33] E. R. MacQuarrie, T. A. Gosavi, N. R. Jungwirth, S. A. Bhave, and G. D. Fuchs, Mechanical Spin Control of Nitrogen-Vacancy Centers in Diamond, *Phys. Rev. Lett.* **111**, 227602 (2013).
- [34] X. L. Hei, P. B. Li, X. F. Pan, and F. Nori, Enhanced Tripartite Interactions in Spin-Magnon-Mechanical Hybrid Systems, *Phys. Rev. Lett.* **130**, 073602 (2023).
- [35] B. Z. Rameshti, S. V. Kusminskiy, J. A. Haigh, K. Usami, D. Lachance-Quirion, Y. Nakamura, C. M. Hu, H. X. Tang, G. E. W. Bauer, and Y. M. Blanter, Cavity magnonics, *Phys. Rep.* **979**, 1 (2022).
- [36] H. Y. Yuan, Y. Cao, A. Kamra, R. A. Duine, and P. Yan, Quantum magnonics: when magnon spintronics meets quantum information science, *Phys. Rep.* **965**, 1 (2022).
- [37] D. Lachance-Quirion, Y. Tabuchi, A. Gloppe, K. Usami, and Y. Nakamura, Hybrid quantum systems based on magnonics, *Appl. Phys. Express* **12**, 070101 (2019).
- [38] S. Zheng, Z. Wang, Y. Wang, F. Sun, Q. He, P. Yan, and H. Y. Yuan, Tutorial: Nonlinear magnonics, *J. Appl. Phys.* **134**, 151101 (2023).
- [39] T. Neuman, D. S. Wang, and P. Narang, Nanomagnonic Cavities for Strong Spin-Magnon Coupling and Magnon-Mediated Spin-Spin Interactions, *Phys. Rev. Lett.* **125**, 247702 (2020).
- [40] D. S. Wang, T. Neuman, and P. Narang, Spin Emitters beyond the Point Dipole Approximation in Nanomagnonic Cavities, *J. Phys. Chem. C* **125**, 6222 (2021).
- [41] D. S. Wang, M. Haas, and P. Narang, Quantum Interfaces to the Nanoscale, *ACS Nano* **15**, 7879 (2021).
- [42] L. Trifunovic, F. L. Pedrocchi, and D. Loss, Long-Distance Entanglement of Spin Qubits via Ferromagnet, *Phys. Rev. X* **3**, 041023 (2013).
- [43] M. Fukami, D. R. Candido, D. D. Awschalom, and M. E. Flatté, Opportunities for Long-Range Magnon-Mediated Entanglement of Spin Qubits via On- and Off-Resonant Coupling, *PRX Quantum* **2**, 040314 (2021).
- [44] I. C. Skogvoll, J. Lidal, J. Danon, and A. Kamra, Tunable anisotropic quantum Rabi model via magnon—spin-qubit ensemble, *Phys. Rev. Applied* **16**, 064008 (2021).
- [45] R. P. Cowburn, Probing antiferromagnetic coupling between nanomagnets, *Phys. Rev. B* **65**, 092409 (2002).
- [46] W. Yu, P. S. Keatley, P. Gangmei, M. K. Marcham, T.

- H. J. Loughran, R. J. Hicken, S. A. Cavill, G. van der Laan, J. R. Childress, and J. A. Katine, Observation of vortex dynamics in arrays of nanomagnets, *Phys. Rev. B* **91**, 174425 (2015).
- [47] H. Wang, J. Chen, T. Yu, C. Liu, C. Guo, H. Jia, S. Liu, K. Shen, T. Liu, J. Zhang, M. A. Cabero Z, Q. Song, S. Tu, M. Wu, X. Han, K. Xia, D. Yu, G. E. W. Bauer, and H. Yu, Non-Hermitian coherent coupling of nanomagnets by exchange spin waves, *Nano Res.* **14**, 2133 (2021).
- [48] Ö. O. Soykal and M. E. Flatté, Size dependence of strong coupling between nanomagnets and photonic cavities, *Phys. Rev. B* **82**, 104413 (2010).
- [49] J. T. Hou and L. Liu, Strong Coupling between Microwave Photons and Nanomagnet Magnons, *Phys. Rev. Lett.* **123**, 107702 (2019).
- [50] C. Berk, M. Jaris, W. Yang, S. Dhuey, S. Cabrini, and H. Schmidt, Strongly coupled magnon-phonon dynamics in a single nanomagnet, *Nat. Commun.* **10**, 2652 (2019).
- [51] S. Kim, Ultrafast magneto-optical measurements for probing magnon-phonon interactions in nanomagnets, *Nat. Rev. Phys.* **4**, 288 (2022).
- [52] W. Xiong, M. Tian, G. Q. Zhang, and J. Q. You, Strong long-range spin-spin coupling via a Kerr magnon interface, *Physical Review B* **105**, 245310 (2022).
- [53] X. L. Hei, X. L. Dong, J. Q. Chen, C. P. Shen, Y. F. Qiao, and P. B. Li, Enhancing spin-photon coupling with a micromagnet, *Phys. Rev. A* **103**, 043706 (2021).
- [54] G. Q. Zhang, Y. P. Wang, and J. Q. You, Theory of the magnon Kerr effect in cavity magnonics, *Sci. China-Phys. Mech. Astron.* **62**, 987511 (2019).
- [55] Y. P. Wang, G. Q. Zhang, D. Zhang, X. Q. Luo, W. Xiong, S. P. Wang, T. F. Li, C. M. Hu, and J. Q. You, Magnon Kerr effect in a strongly coupled cavity-magnon system, *Phys. Rev. B* **94**, 224410 (2016).
- [56] Y. P. Wang, G. Q. Zhang, D. Zhang, T. F. Li, C. M. Hu, and J. Q. You, Bistability of Cavity Magnon-Polaritons, *Phys. Rev. Lett.* **120**, 057202 (2018).
- [57] J. M. P. Nair, Z. Zhang, M. O. Scully, and G. S. Agarwal, Nonlinear spin currents, *Phys. Rev. B* **102**, 104415 (2020).
- [58] R. C. Shen, J. Li, Z. Y. Fan, Y. P. Wang, and J. Q. You, Mechanical Bistability in Kerr-modified Cavity Magnomechanics, *Phys. Rev. Lett.* **129**, 123601 (2022).
- [59] R. C. Shen, Y. P. Wang, J. Li, S. Y. Zhu, G. S. Agarwal, and J. Q. You, Long-Time Memory and Ternary Logic Gate Using a Multistable Cavity Magnonic System, *Phys. Rev. Lett.* **127**, 183202 (2021).
- [60] C. Kong, H. Xiong, and Y. Wu, Magnon-Induced Nonreciprocity Based on the Magnon Kerr Effect, *Phys. Rev. Appl.* **12**, 034001 (2019).
- [61] J. Chen, X. G. Fan, W. Xiong, D. Wang, and L. Ye, Nonreciprocal entanglement in cavity-magnon optomechanics, *Phys. Rev. B* **108**, 024105 (2023).
- [62] G. Q. Zhang, Y. Wang, and W. Xiong, Detection sensitivity enhancement of magnon Kerr nonlinearity in cavity magnonics induced by coherent perfect absorption, *Phys. Rev. B* **107**, 064417 (2023).
- [63] Z. Zhang, M. O. Scully, and G. S. Agarwal, Quantum entanglement between two magnon modes via Kerr nonlinearity driven far from equilibrium, *Phys. Rev. Research* **1**, 023021 (2019).
- [64] G. Q. Zhang, Z. Chen, W. Xiong, C. H. Lam, and J. Q. You, Parity-symmetry-breaking quantum phase transition in a cavity magnonic system driven by a parametric field, *Phys. Rev. B* **104**, 064423 (2021).
- [65] G. Liu, W. Xiong, and Z. J. Ying, Switchable Superradiant Phase Transition with Kerr Magnons, *Phys. Rev. A* **108**, 033704 (2023).
- [66] R. P. Erickson, M. R. Vissers, M. Sandberg, S. R. Jefferts, and D. P. Pappas, Frequency Comb Generation in Superconducting Resonators, *Phys. Rev. Lett.* **113**, 187002 (2014).
- [67] J. P. King, K. Jeong, C. C. Vassiliou, C. S. Shin, R. H. Page, C. E. Avalos, H.-J. Wang, and A. Pines, Room-temperature in situ nuclear spin hyperpolarization from optically pumped nitrogen vacancy centres in diamond, *Nat. Commun.* **6**, 8965 (2015).
- [68] D. Zhang, X. M. Wang, T. F. Li, X. Q. Luo, W. Wu, F. Nori, and J. Q. You, Cavity quantum electrodynamics with ferromagnetic magnons in a small yttrium-iron-garnet sphere, *npj Quantum Inf.* **1**, 15014 (2015).
- [69] Y. Tabuchi, S. Ishino, A. Noguchi, T. Ishikawa, R. Yamazaki, K. Usami, and Y. Nakamura, *Science*, **349**, 405 (2015).
- [70] X. Zhang, C. L. Zou, L. Jiang, and H. X. Tang, Strongly Coupled Magnons and Cavity Microwave Photons, *Phys. Rev. Lett.* **113**, 156401 (2014).
- [71] M. Goryachev, W. G. Farr, D. L. Creedon, Y. Fan, M. Kostylev, and M. E. Tobar, High-Cooperativity Cavity QED with Magnons at Microwave Frequencies, *Phys. Rev. Applied* **2**, 054002 (2014).
- [72] T. Niemczyk, F. Deppe, M. Mariani, E. P. Menzel, E. Hoffmann, G. Wild, L. Eggenstein, A. Marx, and R. Gross, Fabrication technology of and symmetry breaking in superconducting quantum circuits, *Supercond. Sci. Technol.* **22**, 034009 (2009).
- [73] Y. Kubo, F. R. Ong, P. Bertet, D. Vion, V. Jacques, D. Zheng, A. Dréau, J. F. Roch, A. Auffeves, F. Jelezko, J. Wrachtrup, M. F. Barthe, P. Bergonzo, and D. Esteve, Strong coupling of a spin ensemble to a superconducting resonator, *Phys. Rev. Lett.* **105**, 140502 (2010).
- [74] Y. Tabuchi, S. Ishino, T. Ishikawa, R. Yamazaki, K. Usami, and Y. Nakamura, Hybridizing Ferromagnetic Magnons and Microwave Photons in the Quantum Limit, *Phys. Rev. Lett.* **113**, 083603 (2014).
- [75] D. Vitali, S. Gigan, A. Ferreira, H. R. Böhm, P. Tombesi, A. Guerreiro, V. Vedral, A. Zeilinger, and M. Aspelmeyer, Optomechanical Entanglement between a Movable Mirror and a Cavity Field, *Phys. Rev. Lett.* **98**, 030405 (2007).
- [76] M. Boneberg, I. Lesanovsky, and F. Carollo, Quantum fluctuations and correlations in open quantum Dicke models, *Phys. Rev. A* **106**, 012212 (2022).
- [77] A. Angerer, S. Putz, D. O. Krimer, T. Astner, M. Zens, R. Glattauer, K. Streltsov, W. J. Munro, K. Nemoto, S. Rotter, J. Schmiedmayer, and J. Majer, Ultralong relaxation times in bistable hybrid quantum systems, *Sci. Adv.* **3**, e1701626 (2017).
- [78] J. R. Johansson, P. D. Nation, and F. Nori, Qutip: An open-source Python framework for the dynamics of open quantum systems, *Comput. Phys. Commun.* **183**, 1760 (2012).
- [79] J. R. Johansson, P. D. Nation, and F. Nori, Qutip2: A Python framework for the dynamics of open quantum systems, *Comput. Phys. Commun.* **184**, 1234 (2013).
- [80] G. Balasubramanian, P. Neumann, D. Twitchen, M. Markham, R. Kolesov, N. Mizuochi, J. Isoya, J. Achard,

- J. Beck, J. Tessler, V. Jacques, P. R. Hemmer, F. Jelezko, and J. Wrachtrup, Ultralong spin coherence time in isotopically engineered diamond, *Nature Mater.* **8**, 383 (2009).
- [81] H. Fröhlich, Theory of the Superconducting State. I. The Ground State at the Absolute Zero of Temperature, *Phys. Rev.* **79**, 845 (1950).
- [82] S. Nakajima, Perturbation theory in statistical mechanics, *Adv. Phys.* **4**, 363 (1953).